Polyurethane Cascade Depolymerization by a Combination of Thermal Pretreatment and Enzymatic Hydrolysis

ChemSusChem

Chemistry Europe
European Chemical Societies Publishing
ChemSusChem

RESEARCH ARTICLE OPEN ACCESS

Polyurethane Cascade Depolymerization by a Combination of Thermal Pretreatment and Enzymatic Hydrolysis

Shengwei Sun[1,2] | Sathiyaraj Subramaniyan[1,3] | Ganapathy Ranjani[1,2] | Leandro Cid Gomes[4] | Diana Bernin[4] | Thomas Bayer[5] | Uwe T. Bornscheuer[5] | Minna Hakkarainen[1,3] | Per-Olof Syrén[1,2]

[1]School of Engineering Sciences in Chemistry, Biotechnology and Health, Department of Fibre and Polymer Technology, KTH Royal Institute of Technology, Stockholm, Sweden | [2]School of Engineering Sciences in Chemistry, Biotechnology and Health, Science for Life Laboratory, Solna, Sweden | [3]KTH Royal Institute of Technology, Wallenberg Wood Science Center (WWSC), Stockholm, Sweden | [4]Department of Chemistry and Chemical Engineering, Chalmers University of Technology, Göteborg, Sweden | [5]Department of Biotechnology & Enzyme Catalysis, Institute of Biochemistry, University of Greifswald, Greifswald, Germany

Correspondence: Per-Olof Syrén (perolof.syren@biotech.kth.se)

Received: 19 November 2025 | **Revised:** 9 January 2026 | **Accepted:** 12 January 2026

Keywords: enzymatic depolymerization | heat pretreatment | molecular docking | polyurethane | product analysis

ABSTRACT

Enzymatic depolymerization of postconsumer polyurethanes (PURs) offers a promising route for sustainable plastic waste management. However, the complex chemistry of PURs containing carbamate, ether, and ester bonds poses a challenge for such a biotechnological process. Here, we explored the deconstruction of a commercial polyether-polyester-PUR through a cascade depolymerization approach, in which a low-temperature thermal pretreatment (180°C, 4 h) was combined with tandem enzymatic hydrolysis. Heat treatment modified the polymer's physicochemical properties, enabling the cutinase HiC from *Humicola insolens* to cause more than 8% weight loss of the treated PUR films, versus less than 2% of the untreated control after 48 h incubation. Furthermore, the addition of the metagenomic urethanase SP2 completed the one-pot enzymatic cascade, achieving not only depolymerization to the constituent monomer, 4,4′-methylenedianiline (MDA), but also a nearly 3-fold increase in MDA yield compared to using SP2 alone. Docking studies highlighted HiC's specificity toward ester bonds in the PUR polymeric units, and two HiC variants further enhanced degradation within 24 h. Altogether, this work lays the foundation for future investigation and process design for the depolymerization of polyether-polyester-PURs and related materials by cascade enzymatic reactions.

1 | Introduction

Polyurethanes (PURs) serve as important synthetic polymers, featuring urethane bonds derived typically from diisocyanates and polyols [1]. The global market volume of PUR amounted to nearly 25.8 million metric tons in 2022 and is forecasted to grow to >31 million tons by 2030 [2]. PURs can be processed into either thermoplastics or thermosets with superior material properties due to interchain cross-linking. Such structural programmability and facile processability make PURs an attractive choice for various applications, such as binders, adhesives, and sealants (10%), coatings (14%), elastomers (8%), flexible foams (36%), and rigid foams (32%) [3]. While high durability and resistance are considered advantageous properties, the reluctance of PURs to decompose contributes to environmental issues [4, 5]. The disposal and accumulation of PURs can irreversibly damage terrestrial and aquatic ecosystems. To tackle the escalating environmental pollution and avoid plastic waste mismanagement, highly efficient recycling approaches are immensely needed for the recycling of postconsumer PUR [3].

Recently, enzymatic depolymerization of plastics has emerged as a promising method by selectively cleaving the covalent bonds in polymers to release their constituent monomers. Monomeric building blocks can then be used to produce new plastics (closed-loop recycling) or other value-added products (open-loop

recycling), realizing a circular plastic economy [6]. A number of hydrolases, including cutinases, esterases, lipases, and proteases, have been reported to catalyze the hydrolysis of the ester bonds present in PURs, for example [7]. However, the enzymatic degradation performance is often low and constrained by the complex composition and formulations of PURs [1, 8], especially their highly stable urethane unit with bond dissociation energies of ca 80 kcal/mol for N–C and 90 kcal/mol for C–O) [9], and the presence of additional ether segments. Polyols are an essential component of many PURs, which expand their versatility further by generating either polyester or polyether-type materials. Polyester-based PURs usually show higher strength, solvent resistance, and abrasion resistance, whereas polyether-based PURs often offer hydrolytic stability and better durability [10]. Integrating both ester and ether segments can create high-performance materials, offering a wide range of applications [11], such as the waterborne PUR films and coatings [12, 13]. Still, depolymerization of polyether-polyester-based PURs remains essentially unexplored.

In previous studies, polyester-based materials such as the commercial Impranil DLN have received significant attention as model substrates for enzymatic hydrolysis of PUR (Figure 1, top left) [18–21]. Impranil DLN is a polyester PUR dispersion, lacking the aromatic amines characteristic of many PURs [22]. Other polyester-based PUR materials analyzed in enzymatic hydrolysis studies have included poly (butylene adipate) (PBA)-based PUR and thermoplastic polyester-PUR (TPU) foams, exhibiting good flexibility and high elasticity (Figure 1). While these polyester PURs are generally more susceptible to degradation through the cleavage of confined ester bonds [23–26], the hydrolysis of polyether-based PUR to produce the constituent monomers has not been achieved until recently, with the discovery of three urethanases SP1, SP2, and SP3 from a metagenomic library [16]. Notably, SP2 was able to break down the urethane bonds in low-molecular-weight carbamates within a toluene diisocyanate (TDI)-based polyether-PUR to release the monomeric aromatic diamines (toluene-2,4-diamine and toluene-2,6-diamine). Following glycolysis at 200°C, using an excess of diethylene glycol (DEG) containing tin (II)-2-ethylhexanoate as a catalyst, SP2 could also produce monomeric 4,4′-methylenedianiline (MDA) from pretreated methylene diphenyl diisocyanate (MDI)-based polyether-PUR [17]. A QM/MM-based mechanistic study has recently provided a deep insight into the urethanase SP2 catalyzing the degradation of the urethane bond in a model compound [27]. However, challenges remain with regard to the selection of a suitable catalyst and alcohol reagent to implement the glycolysis, which not only may affect the hydrolysis efficiency but could also inactivate enzymes during the coupled process [28]. A mild, simple, efficient, green, and sustainable method for PUR depolymerization is still highly desirable.

Recently, we have introduced the concept of chemoenzymatic cascade depolymerization of plastics, in which chemical pretreatment under mild conditions precedes biocatalytic depolymerization of generated shorter-chain fragments to induce selectivity in the upcycling process [29]. In this study, we investigated the feasibility of cascade depolymerization of a commercially available polyether-polyester-based PUR by thermal pretreatment in the absence of any solvent, followed by a two-enzyme cascade comprising the cutinase HiC and the urethanase SP2. Material characterization of PUR before and after the heat treatment, using a panel of spectroscopy methods, the determination of weight loss of PUR upon enzymatic depolymerization, and the identification of degradation products were performed. Furthermore, an in silico docking study was used to understand the key amino acid residues responsible for interactions with models of the PUR

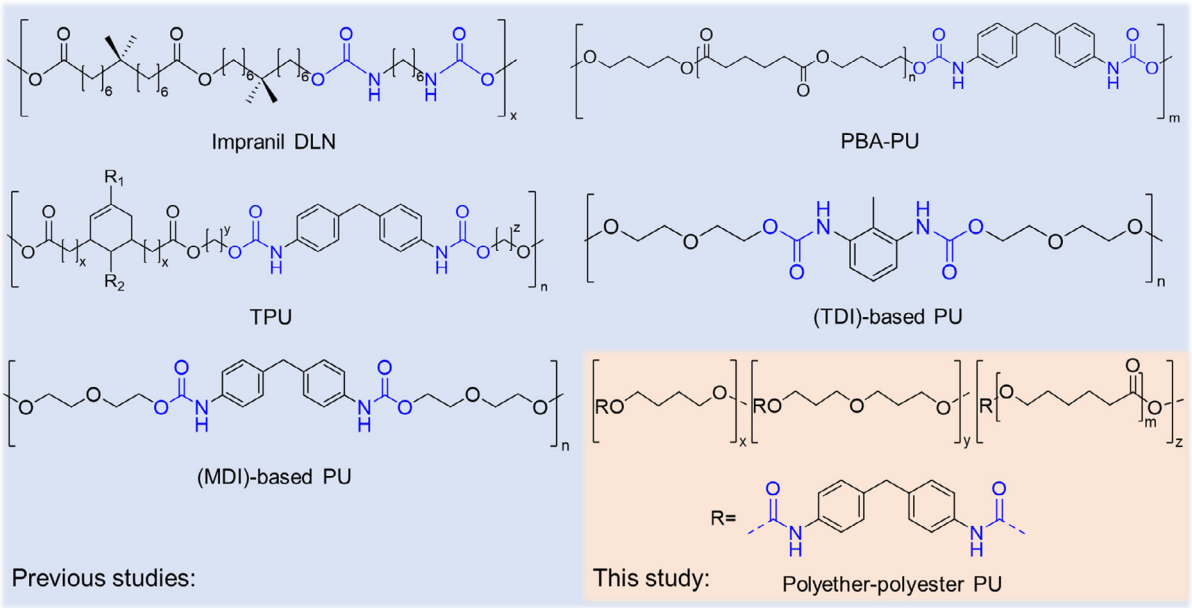

FIGURE 1 | PUR substrates for enzymatic hydrolysis used in previous works and this study. Impranil DLN is an anionic aliphatic polyester-PUR dispersion, which is produced by Covestro AG (Leverkusen, Germany). PBA-PUR was chemically synthesized by Liu et al [14]. TPU was obtained from Soprema (Strasbourg, France) based on a custom synthesis using a fatty acid-derived polyester polyol [15]. TDI-based PUR was provided by a local manufacturer [16], and MDI-based PUR was obtained from Dongguan Jintian Plastic Materials Co., Ltd., Guangdong, China [17]. Polyether-polyester-PUR (Poly[4,4′-methylenebis(phenyl isocyanate)-alt-1,4-butanediol/di(propylene glycol)/polycaprolactone]), used in this study, was bought from Sigma–Aldrich (St. Louis, USA). The urethane units are colored in blue in all PUR materials.

substrate employed. Finally, two HiC variants with enhanced enzyme activity were used to hydrolyze the heat-treated PUR. Together, this study provides a simple, sustainable, and highly effective strategy for PUR deconstruction by cascade depolymerization [29] based on a combination of thermal pretreatment and enzymatic hydrolysis.

2 | Experimental Section

2.1 | Materials and Reagents

The polyether-polyester-PUR (pellets, product No. 430 218, CAS No. 68 084-39-9, 1.18 g/mL density at 25°C) was bought from Sigma–Aldrich (St. Louis, USA). Organic solvents, including dimethylformamide (DMF), tetrahydrofuran (THF), and acetonitrile (ACN), were bought from Sigma–Aldrich (St. Louis, USA). 4,4′-Methylenedianiline (MDA) (white powder, product No. 32 950, purity ≥97.0%) was purchased from Sigma–Aldrich (St. Louis, USA), as well as kanamycin, imidazole, and isopropyl β-D-1-thiogalactopyranoside (IPTG). Tryptone, yeast extract, and NaCl for preparing cell culture medium were bought from VWR International (Pennsylvania, USA).

2.2 | Thermal Treatment of PUR

Approximately 380 mg PUR pellets (~3 × 2 × 2 mm) were weighed and filled in a glass vial (2.5 × 6.5 cm), which was then placed in an oil bath for temperature control. Thermal treatment of PUR was conducted in a fume hood at 180°C for 4 h with air circulation [30]. After heat treatment, PUR samples were allowed to cool down to room temperature, then collected and shredded into small granules (~0.5 × 0.5 × 0.5 mm).

2.3 | Characterization of PUR Materials

Thermogravimetric analysis (TGA) was conducted using a Mettler Toledo TGA 1 (Greifensee, Switzerland). Around 7.65 mg of PUR pellets were placed into TGA crucibles and heated at a temperature of 180°C for 4 h with a heating rate of 10°C/min at an air flow rate of 50 mL/min. TGA crucibles without samples were used as a blank control.

Ultraviolet–visible (UV–Vis) spectroscopy scanning was performed using a microreader (SpectraMax iD3, California, USA) at room temperature. PUR samples (2 mg) before and after heat treatment were dissolved in 1 mL DMF overnight. Around 150 µL of this PUR solution was added to the 96-well plate (Greiner, Merck), and then the UV absorbance was monitored at a wavelength of 230–400 nm.

Size exclusion chromatography (SEC) was performed on a TOSOH EcoSEC HLC-8320 GPC system (Tokyo, Japan) equipped with an EcoSEC RI detector and three columns (PSS PFG 5 µm; Microguard, 100, and 300 Å) from PSS GmbH with M_w resolving range: 100–300,000 g/mol. DMF as solvent with 0.01 M LiBr was used as the mobile phase at 50°C with a flow rate of 1 mL/min. Poly (methyl methacrylate) (PMMA) standards between 700 and 2,000,000 g/mol were used for the calibration. The injection volume of PUR samples (3 mg/mL) was set to 20 µL.

Differential scanning calorimetry (DSC) measurements were performed using a Mettler Toledo DSC 1 instrument (Greifensee, Switzerland). Approximately 5 mg of PUR samples were placed in 40 µL aluminum cups. The samples were then heated from 25 to 300°C with a heating rate of 10°C/min at a nitrogen (N_2) flow rate of 50 mL/min.

Fourier transform infrared spectroscopy (FTIR) was carried out with a PerkinElmer 100 spectrometer (Massachusetts, USA) equipped with an attenuated total reflection (ATR) setup. For all the PUR samples, 16 successive scans over the range of 400–4,000 cm^{-1} were performed. The background scan was acquired without a sample present.

Scanning electron microscope (SEM) images were taken using a FEI Quanta 200 FEG ESEM instrument (Oregon, USA). The PUR film samples were coated with gold before the SEM analysis to increase image quality. Images of the sample with different magnifications were recorded at 10.0 kV using an Everhart-Thornley detector (ETD) as a secondary electron (SE) detector.

2.4 | Enzyme Production and Purification

Chemically competent *Escherichia coli* C43 (DE3) were transformed with plasmids containing the genes encoding HiC, HiC mutants, and SP2 by established heat-shock protocols (for GenBank IDs, see Supporting Information). Fresh lysogeny broth (LB) medium (5 mL; 10 g/L tryptone, 5 g/L yeast extract, and 10 g/L NaCl) containing 50 µg/mL kanamycin was inoculated with the desired *E. coli* C43 (DE3) transformant and then incubated at 37°C with 180 rpm shaking overnight. After incubation, 1 mL bacterial solution was added to a fresh 100 mL LB culture medium supplemented with the same concentration of antibiotic. The cell cultures were incubated at 37°C for 2–3 h until the optical density measured at 600 nm (OD_{600}) reached 0.6–0.8. Subsequently, 1 mM IPTG was added to the medium to induce protein production. After incubation at 18°C for 24 h, the cell pellets were harvested by centrifugation at 4,000 *g* and 4°C for 10 min. They were then resuspended in 20 mL Tris-HCl buffer (25 mM, pH 7.5) and lysed by sonication (45% power, 2 s pulse and 4 s off). The crude cell lysates containing enzymes were obtained after centrifugation at 4,000 *g* for 20 min. The ÄKTA pure protein purification system (GE Healthcare, Illinois, USA) equipped with 1 mL HisTrap HP prepacked columns (Cytiva, Amersham, UK) was used to purify enzymes of interest. Tris-HCl buffers (25 mM, pH 7.5) containing 20 and 250 mM imidazole were used to wash HisTrap columns and elute the target enzymes, respectively. PD-10 columns (Cytiva, Amersham, UK) were used to desalt the protein samples against Tris-HCl buffer (25 mM, pH 7.5) as instructed by the manufacturer. Concentration of protein samples was measured using a NanoDrop Spectrophotometer (VWR, Pennsylvania, USA), and purity was examined by SDS-PAGE (Figure S1). Purified enzyme solutions were stored at 4°C.

2.5 | Enzymatic Hydrolysis of PUR Films

For the enzymatic hydrolysis assay, different weights of PUR granules before and after heat treatment were dissolved in 20 mL THF to prepare 2.5, 5, 7.5, 10, and 15 mg/mL PUR films. The polymer solution was cast in a 9 cm glass petri dish and was

then left in the fume hood for the organic solvent to evaporate overnight. The films were cut into pieces of ~1 × 1 cm^2. Both untreated and heat-treated PUR films were then incubated in 500 μL Tris-HCl buffer (25 mM, pH 7.5) containing 20 μg purified enzymes at 50°C and 180 rpm for 24 h. After reaction, these films were washed three times with MilliQ water and dried at 50°C until the weight did not change. The weight loss before and after incubation was recorded to determine the extent of enzymatic degradation. The representative films were photographed to compare the enzymatic degradation of untreated and heat-treated PUR. Furthermore, the weight loss of 15 mg/mL PUR films was measured with an increase in time up to 48 h. For the enzymatic cascade degradation, PUR films (particle loading of 15 mg/mL) were incubated with 20 μg HiC in 500 μL Tris-HCl buffer solution (25 mM, pH 7.5) at 50°C for 24 h, followed by adding 20 μg purified SP2 into the reaction solution, which was incubated at 30°C and 180 rpm for another 24 h. The films incubated with 20 μg single HiC or SP2 at 50°C or 30°C for 48 h were used as control groups. Samples without any addition of enzymes were set up as a blank control group.

2.6 | Analysis of the Degradation Product by High-Performance Liquid Chromatography-Mass Spectrometry (HPLC-MS)

After the enzymatic degradation, 500 μL reaction solution was pipetted into a new 1.5 mL Eppendorf tube. An equal volume of cold acetonitrile (500 μL) was added to stop the reaction and increase the solubility of the products. Samples of untreated and heat-treated PUR films were filtered through a 0.22-micron pore size syringe filter before being submitted to HPLC-MS (Agilent 1260 Infinity II, USA). An X-bridge C18 column (50 × 3.0 mm, 3.5 μm) was used to separate the products in the reaction mixture. Mobile phases including acetonitrile (A) and 10 mM NH_4HCO_3/H_2O (B) were used under the 20%–97% gradient elution within 10 min. The injection volume was 2 μL. The flow rate was set to 1 mL/min. The UV absorbance of products was monitored using a diode array detector. The MS data was collected under the default setup of the instrument. The quantification of MDA was performed based on the standard curve (peak area vs. concentration ranging from 0.0005 to 5 mM, Figure S2).

2.7 | Molecular Docking

Autodock Vina (v1.1.2) [31] was used to analyze the interaction between three building blocks of PUR and the cutinase HiC. The protein structure (PDB ID: 4OYY) was downloaded from the protein data bank (https://www.rcsb.org/), while three ligand structures were prepared using ChemDraw (v23.1.1), which were structurally optimized using Avogadro (v1.1.0) [32] and exported in PDB format. Before running final docking, ligands were prepared by adding polar hydrogens and assigning Gasteiger charges. Rotatable bonds were defined to allow full ligand flexibility, and AutoDock-specific atom types were assigned; ligand files were converted to the required PDBQT format. Autodock Tools (v1.5.6) [33] were then employed for docking substrates into the active pocket of the enzyme. The grid box with a size of 40 × 40 × 40 Å was centered in the catalytic residues of the S105-D160-H173 motif. The Lamarckian Genetic Algorithm (LGA) was employed to search for the best conformers. All other parameters were set to default values. The ligand conformations with the lowest binding energy calculated by AutoDock's scoring function were selected as the best-docked pose (Table S1). The generated complex of receptor and ligand was exported for further analysis by visual inspection.

3 | Results and Discussion

3.1 | Characterization of the PUR Materials

Thermal depolymerization, such as pyrolysis, has been widely used for plastic recycling. These processes are carried out under elevated temperatures (450°C–800°C) and are amenable for unspecific scission of polymer chains into fuels and other chemical products, instead of the original monomers [34]. Solvolysis, such as hydrolysis, glycolysis, and alcoholysis, is suited for recycling a wide range of condensation plastics. A closed-loop recycling process for polyurethane was also demonstrated, where the recovered polyols and isocyanates could be reused to produce new PUR products [35]. Yet, challenges remain regarding the economic cost of processing and technical complexity, as well as the generation of by-products and residual wastes. In contrast, thermal/heat treatment under relatively low-temperature exposure has been demonstrated as a viable route of plastic decomposition, which can also change the physicochemical properties of polymer materials and enhance enzyme accessibility, facilitating further depolymerization [36]. Here, we hypothesized that heating the PUR would result in altered material secondary structure and reduced molecular weight to enhance accessibility for the biocatalyst.

After applying relatively low-temperature heat pretreatment (180°C for 4 h) in the absence of organic solvents and additional catalysts, changes in the properties of polyether-polyester-based PUR could be observed. Solubility tests showed that the heat-treated PUR displayed a significant reduced solubility, with many insoluble polymer fragments formed, whereas the untreated material was dissolved well in the THF solution (~95% estimated solubility, Figure S3). This might be attributed to the reaction of residual functional groups (e.g. isocyanates), with urethane or hydroxyl functionalities under heating conditions, leading to the formation of allophanate-type crosslinks in the PUR [37]. Isothermal TGA analysis showed that the weight of PUR pellets only slightly decreased from 7.65 to 7.63 mg (Figure 2a) during this treatment, indicating that this PUR polymer has a high thermal stability, and purely thermal degradation would require harsher conditions. UV spectroscopy performed in DMF yielded two peaks with increased absorbance around 260–290 nm and 310–320 nm after the heat-treatment process (Figure 2b), which might correspond to the C=O and N–H in the chromophores formed by increased molecular movement, bond scission, and oxidation in the PUR material [38]. SEC indicated that the molecular weight decreased by nearly half (from 160,900 to 80,240 g/mol) (Figure 2c), while DSC analysis showed that the melting temperature (T_m) (from 215–205°C) and glass transition temperature (T_g) (from –40°C to –45°C) decreased post pretreatment (Figure 2d,e). This can be explained by the reduced molecular weight and increased mobility of the polymer chains [39]. FTIR showed the characteristic peaks of both N–H and C–H

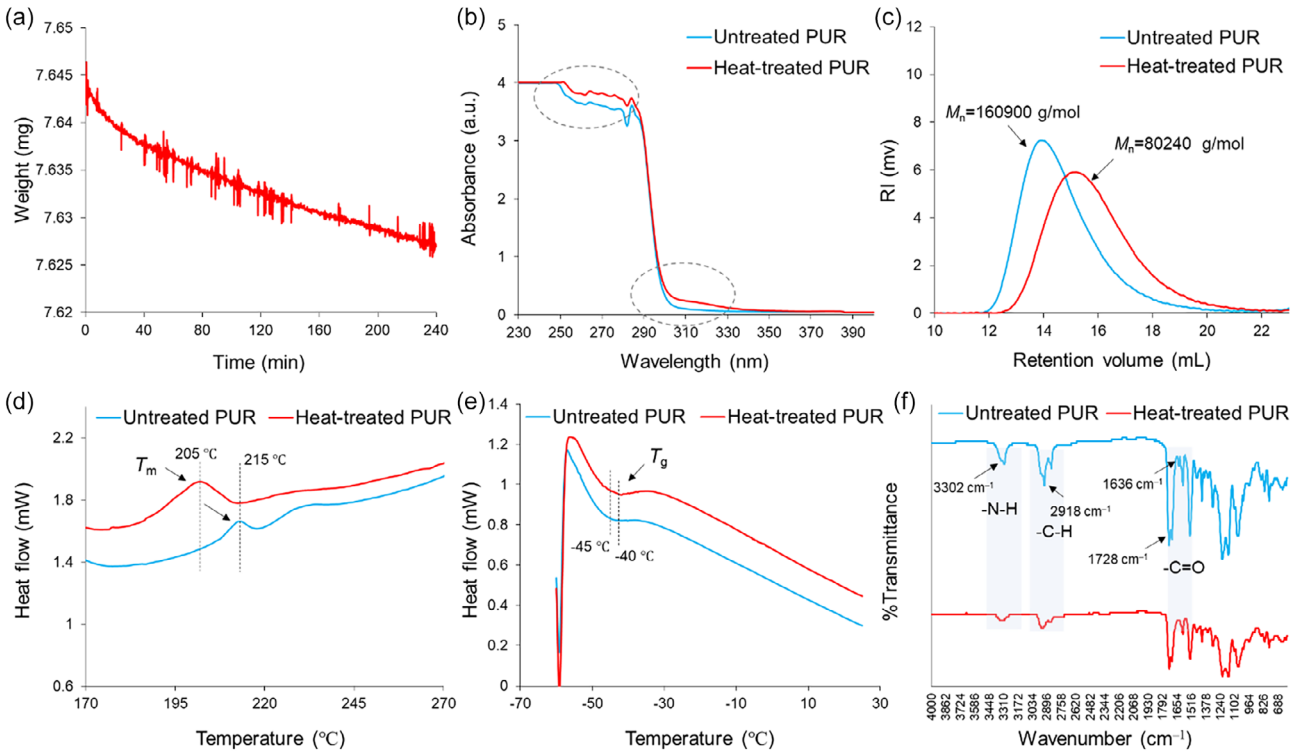

FIGURE 2 | Characterization of the commercial PUR material before and after heat treatment. (a) Isothermal TGA analysis. (b) UV spectroscopy. (c) SEC analysis. (d) DSC measurement of T_m values (endo up). (e) DSC measurement of T_g values (endo up). Data collected during first heating cycle. (f) FTIR determination of untreated and heat-treated PUR.

stretching at 3 302 and 2 918 cm^{-1}, which indicated the presence of urethane linkages within the polymer structure and aliphatic chains in the soft segments of PUR, respectively. After heat treatment, these two peaks became broadened and lost sharpness (Figure 2f). This is a typical indicator of thermal degradation involving chemical bond breaking and a decrease in the abundance of the chemical groups. The split peak of the C=O group, typically around 1,720 and 1,705 cm^{-1}, indicates the presence of both free and hydrogen-bonded urethane carbonyl groups in the PUR, respectively [40]. The stretching vibration peak at 1,636 cm^{-1} could be attributed to the urea C=O group that is connected to N–H via hydrogen bonding [41]. The disappearance of this peak suggested that bond or network breaking and polymer chain scission occurred during the heating process (Figure 2f). This is consistent with the reduced molecular weight of PUR polymer observed before (Figure 2c), which plays an important role in the degradation of plastic polymers and copolymers by microorganisms and corresponding enzymes [42–44].

Philipp et al. studied the changes in the molecular weight of thermoplastic polyether- and polyester-based PURs under thermal, hydrolytic, and UV degradation conditions for 14 days [30]. They also found that a rapid decrease in the molecular weight of both types of PURs occurred when exposed to elevated temperatures (≥175°C). Similarly, Gallorini et al. used hydrothermal liquefaction (supercritical water at 250°C–400°C) as a thermal pretreatment of a commercial polyester-based PUR before enzymatic degradation [45]. By using FTIR, they identified the N–H stretching band at 3,309 cm^{-1}, and the aromatic and aliphatic C–H stretching at around 3,000 cm^{-1}, in line with our spectra.

3.2 | Enzymatic Degradation of PUR Films

Next, we performed the enzymatic degradation of PUR films, prepared from the polyether-polyester-PUR, before and after heat pretreatment. Cutinases (EC 3.1.1.74), belonging to the α/β-hydrolase fold superfamily, and have been well-documented regarding their ability to catalyze the hydrolysis of synthetic polyesters [46]. For example, the cutinase HiC from *Humicola insolens* (*H. insolens*) has been reported to hydrolyze poly(butylene succinate) (PBS), poly(butylene succinate-co-adipate) (PBSA), poly(ε-caprolactone) (PCL), and poly(butylene adipate-co-terephthalate) (PBAT) [47]. Notably, HiC is recognized as a promising biocatalyst for the hydrolysis of (pretreated) PET [48–50]. Targeting the ester moiety in a polyester-polyurethane copolymer by HiC reduced its molecular weight by 42%–84% and resulted in cracks on the surface of the corresponding polymer films after incubation at 50°C for 168 h [51]. For these reasons, we selected HiC as the model enzyme for ester bond hydrolysis in this study.

Accordingly, purified HiC caused visible damage to the polyether-polyester-based PUR films after incubation at 50°C for 24 h (Figure 3a). We assessed the effect of different polymer particle loadings (from 2.5 to 15 mg/mL) after shredding on the degradation efficiency of the investigated PUR films, as differences in particle loadings can significantly affect the efficacy of degradation due to altered accessible surface area as well as film performance [52]. At particle loadings ≥5 mg/mL, no damage to PUR films could be observed without heat pretreatment. In contrast, the cutinase HiC caused obvious damage to the heat-treated PUR films, which were broken down into small pieces even at the highest particle concentration of 15 mg/mL after 24 h incubation

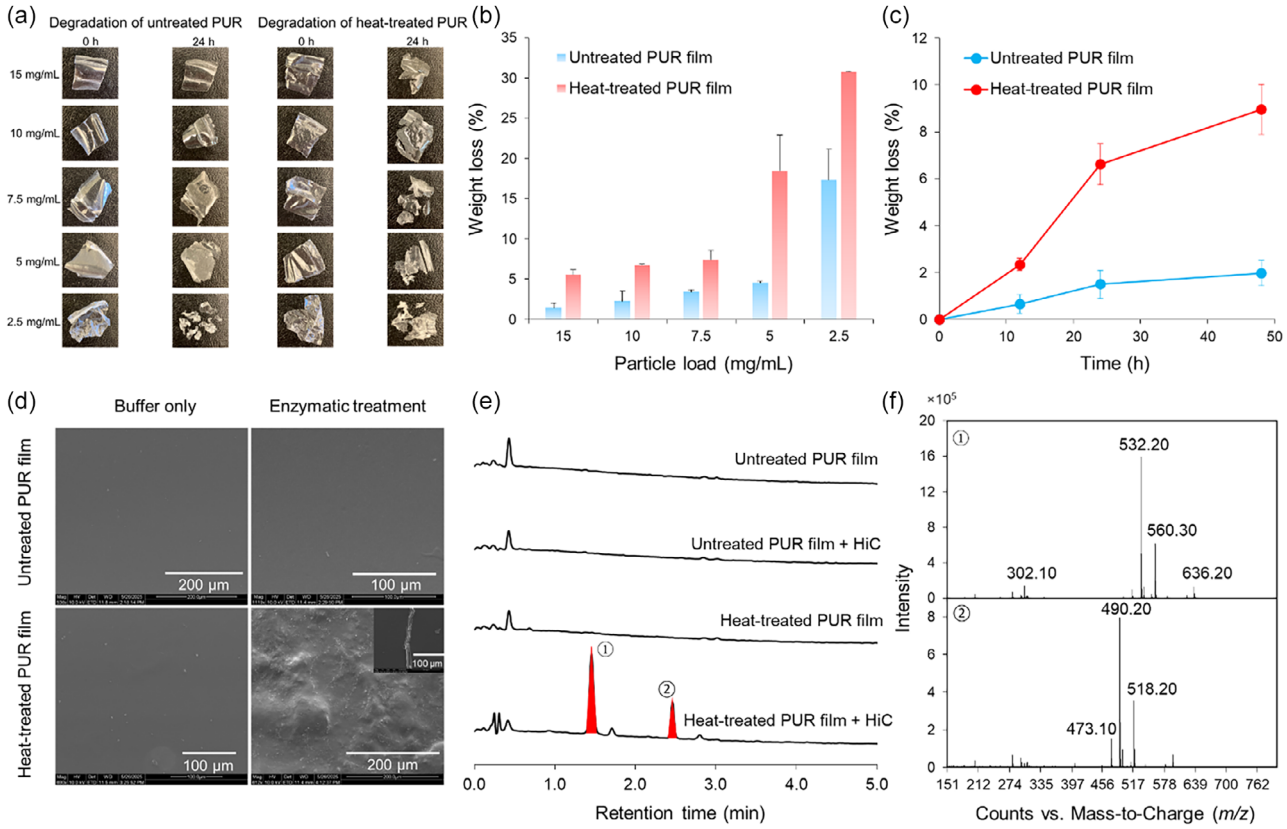

FIGURE 3 | Enzymatic degradation of PUR films using *H. insolens* cutinase (HiC). (a) A comparative study of the enzymatic degradation of untreated and heat-treated PUR films with different particle loadings after 24 h reaction at 50°C. The reaction system comprises the same weight (~10 mg) of PUR films with a similar shape and 20 μg of enzyme in 25 mM Tris-HCl buffer (pH 7.5). (b) Weight loss of PUR films after 24 h incubation. (c) Weight loss of PUR films (particle load: 15 mg/mL) with time. (d) SEM of untreated and heat-treated PUR films with and without enzymatic treatment for 48 h. For the heat-treated PUR film, wrinkled bulges and small cracks (lower right corner) were observed after incubation with the enzyme. (e) HPLC spectra of released products from PUR films (particle load: 15 mg/mL) at 50°C for 24 h with and without pretreatment and enzyme, respectively. (f) Mass spectra of the two major peaks (① and ②) of the highest intensity with *m/z* of 532.20 (①) and 490.20 (②).

(Figure 3a). Moreover, significantly higher weight loss was recorded for heat-treated PUR films compared to the untreated films (Figure 3b). It was found that the lower the particle loading, the greater the mass loss for both untreated and heat-treated PUR films. Notably, HiC caused more than 8% weight loss of heat-treated PUR film (15 mg/mL) while less than 2% of the untreated control was recorded after 48 h incubation (Figure 3c). The lost portion may respond to the formation of microplastics, nanoplastics, or new products (see below). The improved enzymatic degradation efficiency can be explained by the changes in the structural properties described above after heat treatment. Beyond reduction of molecular weight, thermal treatment can increase chain mobility in PUR elastomers, promoting hard–soft segment reorganization and postcuring reactions that lead to covalent crosslinking. In the polyether-polyester-PUR system under study, heat-induced ester linkage interchange together with increased phase separation, reduced degree of polymerization, and altered surface morphology can expose or generate more enzyme-accessible ester groups; thereby enhance enzymatic degradation despite increased crosslinking. We also found that a higher particle loading correlated with the increasing thickness of the plastic films (Figure S4). The thickness of untreated PUR films was generally higher than that of heat-treated PUR films, contributing to lower enzymatic degradation. This is in agreement with the biodegradation of PET films reported before [53]. SEM images demonstrated wrinkled bulges and cracks on the surface of heat-treated PUR films subjected to the enzyme, whereas no obvious changes were seen on the untreated PUR films after 48 h incubation (Figure 3d). Overall, these data suggest that HiC exhibits increased degradation activity against the investigated PUR material after heat pretreatment.

To complement the weight-loss experiments, putative degradation products from enzymatic depolymerization of polyether-polyester-PUR films were analyzed by HPLC-MS. Two major peaks from heat-treated PUR film were found in the spectra using UV-detection, but not in the corresponding spectra from the untreated PUR films (Figure 3e). Based on the mass spectrum, these two peaks showed *m/z* at 532.2 and 490.2 (Figure 3f). We reason that HiC breaks down the ester bonds in the PUR, releasing compounds or oligomers ① and ②, demonstrating the activity of HiC on ester bonds in the investigated polyether-polyester-PUR. Interestingly, a previous report demonstrated that the cutinase HiC preferentially hydrolyzed ester bonds in a polyester-based PUR, while release of the MDA

monomer was deteced according to liquid chromatography time-of-flight/mass spectrometry (LC-MS-TOF) [51]. In contrast, and as expected for a cutinase acting only on ester bonds, we only observed the possible hydrolysis of ester bonds in the polyether-polyester-based PUR, releasing compounds ① and ② in this study.

The absence of MDA formation after single HiC degradation is likely because the enzyme is not active on urethane bonds compared to ester bonds which the enzyme can readily hydrolyze [51]. We also took this observation as a sign that the complex structure of the PUR material used in this study might hinder enzymatic depolymerization by limiting enzyme access to the substrate. Indeed, this type of polyether-polyester-PUR has excellent transparency, chemical resistance, flexibility, and toughness, making it a durable and wear-resistant high-performance elastomer with a wide range of applications. For example, it can be used as a shape memory polymer and a reinforcing material to enhance the mechanical and thermal properties. This specific PUR has good biocompatibility and supports endothelial cell proliferation. It incorporates PCL (see Figure 1), which contributes to its biodegradability, as numerous enzymes, particularly esterases and cutinases, are known to catalyze PCL degradation [54]. The built-in PCL can also improve the hydrophobicity of the polymer matrix and can be used to prepare PUR membranes for effective gas separation [55] and to synthesize biomedical hydrogels with good thermodynamic properties [56]. Therefore, more degradation studies are needed to address the potential issues of such PUR plastic waste accumulation in both clinical and natural environments. In fact, most cutinases only have ester bond hydrolysis activity, while a small number of cutinase shows the promiscuous capability of amide or urethane bond hydrolysis (e.g., amide bonds in polyamide 6.6) [57]. To unleash the full potential of cutinases, an enzyme engineering strategy could be used for creating durable and effective biocatalysts.

In addition to HiC, a number of novel cutinases, such as BaCut1 [58], CpCut1 [59], and PlCut1 [60] have been identified from various microorganisms, exhibiting ester bond-degrading activity in PURs. However, either Impranil DLN or polyester-based PUR (e.g., PBA-PUR) was commonly used as a substrate in these studies, which are generally more susceptible to enzymatic depolymerization [61, 62] due to scission of their ester bonds. A direct degradation of polyether- or two-component-based PUR materials remains challenging due to the inertness of the ether bonds and the urethane unit, as well as the structural complexity of these substrates. Viable strategies targeting plastic to chemical recycling of polyether-polyester-PURs could

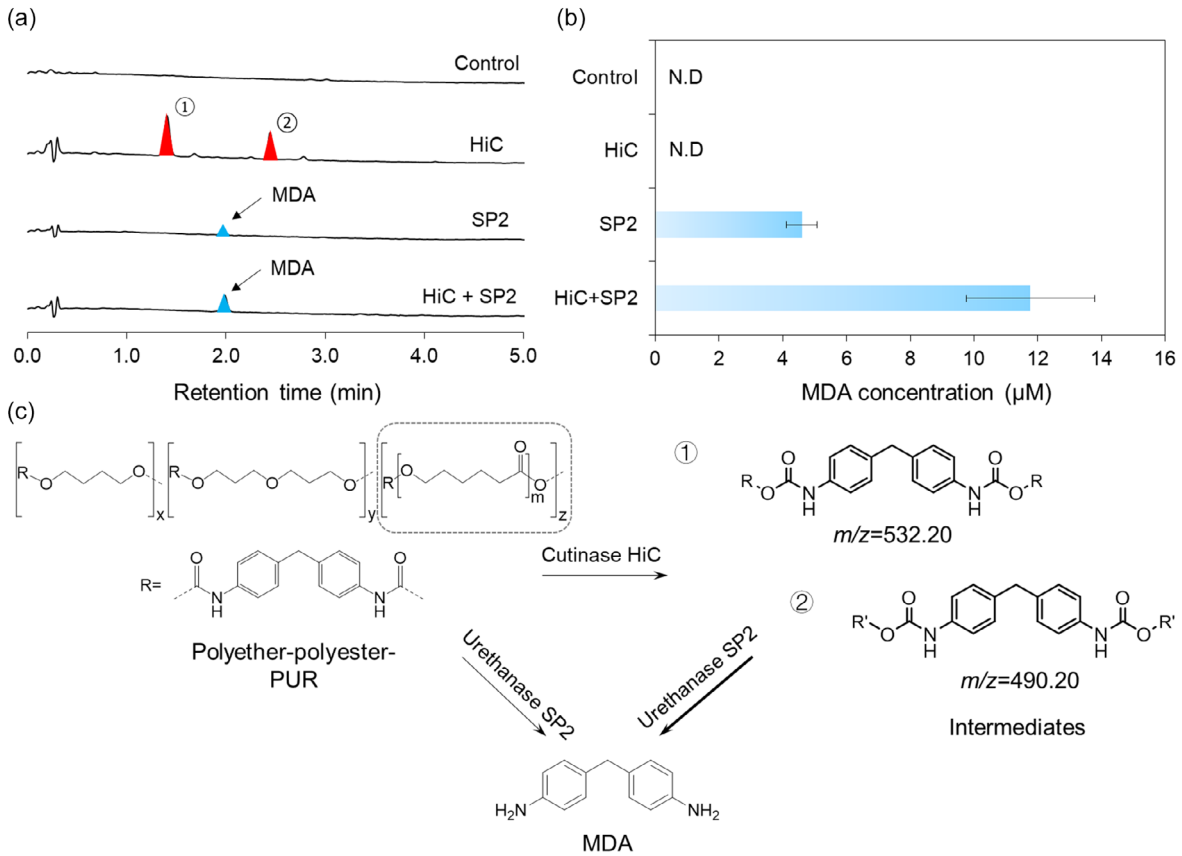

FIGURE 4 | HPLC-MS analysis of degradation products of PUR films. (a) Two-enzyme cascade degradation of heat-treated PUR films to produce monomer MDA. After incubation with HiC for 24 h, 20 μg purified SP2 was added and incubated at 30°C for another 24 h. Simultaneously, a single SP2 of 20 μg was added to the reaction in the absence of HiC at 30°C for 48 h. The MDA is confirmed by the commercial standard (Figure S2). (b) Quantification of MDA concentration after enzymatic degradation. N.D: product not detected. (c) Proposed cascade depolymerization pathway of PUR. Two compounds (① and ②) with *m/z* of 532.20 and 490.20 were obtained by hydrolyzing the ester bonds in PUR (dotted box), followed by hydrolysis of urethane bonds to yield monomer MDA. R and R' indicate different side chains attached to the diamine-based backbone. The bold line indicates the higher conversion efficiency observed for tandem biocatalysis using cutinase concomitant with urethanase.

include cascade depolymerization in conjunction with enzyme engineering.

3.3 | Enzymatic Cascade Depolymerization of PUR to MDA

Scaled-up reactions were performed, attempting to isolate the above-mentioned compounds (① and ②). Unfortunately, sufficient amounts for nuclear magnetic resonance (NMR) analysis could not be obtained. We noted that the *m/z* peak of compound ① at 532.20 could correspond to an oligomer with R equal to 6-hydroxyhexanoic acid (Figure S5), whereas the structure of compound ② with an *m/z* value of 490.20, is difficult to infer. Accordingly, we then explored whether there are urethane bonds present in compounds ① and ② that could be further hydrolyzed by a recently reported urethanase [16]. The urethanase SP2 was recombinantly produced in *E. coli*, purified, and then added to the reaction system to explore if the monomer 4,4′-methylenedianiline (MDA) could be produced through the hydrolysis of urethane bonds. As expected, we found that the proposed intermediates ① and ② could be transformed into MDA in the presence of HiC and SP2 enzymes (Figure 4a). Moreover, 4.6 μM MDA was released when heat-treated PUR films (particle load: 15 mg/mL) were incubated solely using SP2, while 11.7 μM MDA was obtained upon successive incubation with HiC and SP2 (Figure 4b). No detectable amounts of MDA were released from control PUR films or films aged with HiC. A possible degradation pathway based on HPLC analysis and accounting for detected UV-active peaks is proposed in Figure 4c, where the PUR material can be degraded into its monomer MDA at a high concentration through a two-enzyme cascade depolymerization. A similar enzymatic cascade depolymerization by the amidase GatA250 and the leaf-branch compost cutinase (LCC) resulted in a 1.8 time increase in the production of MDA from a polyester-based PUR [63]. In comparison, around 3 μM MDA monomer was produced when a model TPU (particle load: 0.2 mg/mL) was incubated with single urethanase SP1 (1 mg/mL) [15].

When it comes to dual enzyme catalysis, this technique has already been widely applied for PET depolymerization. For example, Knott et al. reported a dual enzyme system (PETase and MHETase from *Ideonella sakaiensis*) for deconstructing PET by utilizing one enzyme to first convert the polymer into more soluble intermediates and another enzyme to produce monomers, indicating that nature has developed similar

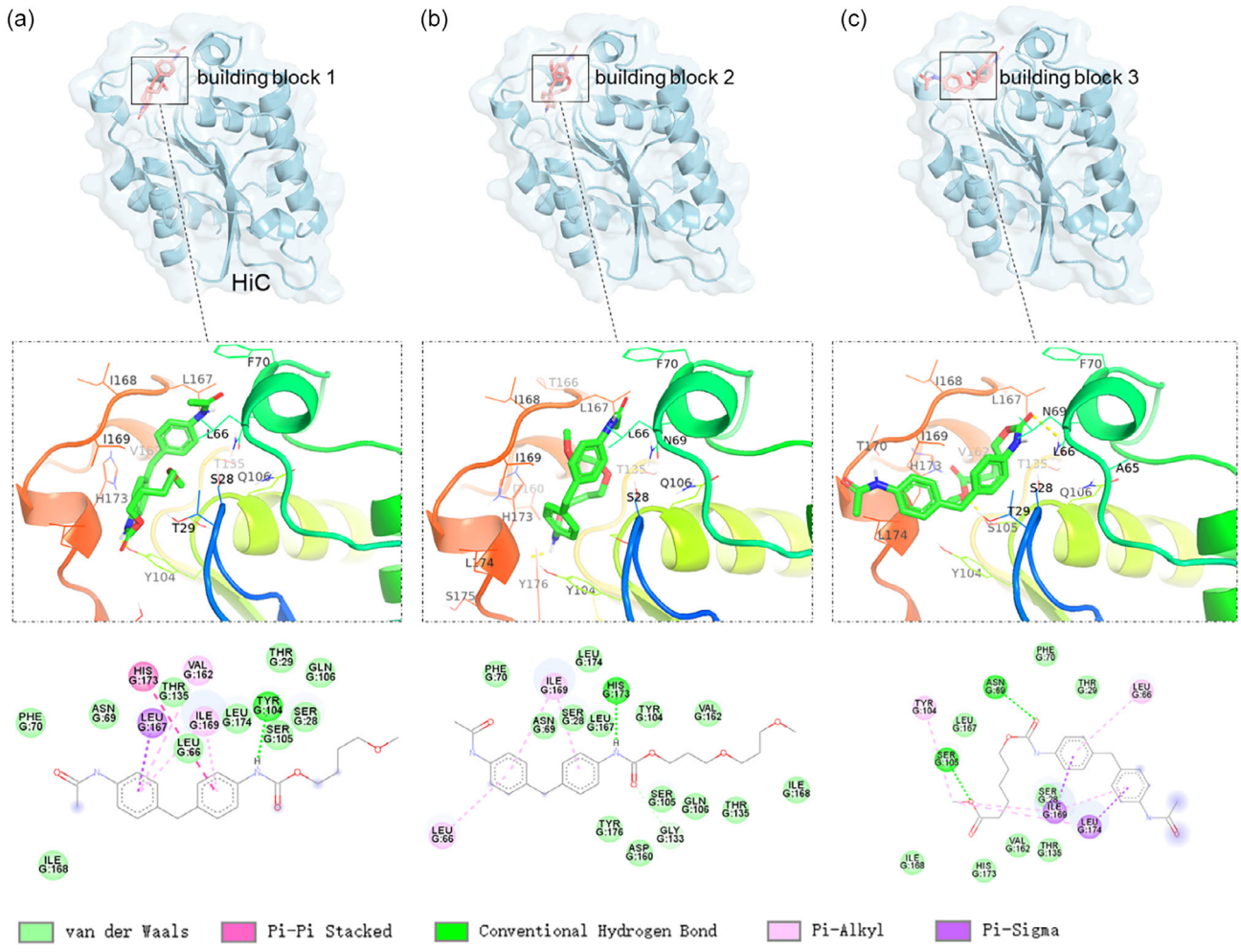

FIGURE 5 | Docking study of HiC against three building blocks. Three different types of repeating units, named building block 1 (a), building block 2 (b), and building block 3 (c), were docked into the active pocket of HiC. The best poses were selected for protein–ligand interaction analysis. Note: residues labeled with "G" are L-type amino acids.

deconstruction strategies for synthetic plastics [64]. Sun et al. engineered a two-enzyme system containing a robust cutinase (HRC) for the first-step PET depolymerization and an esterase PCEST (*Pyrobaculum calidifontis* VA1) for decomposing the PET intermediate product [65]. The synergistic activity of the HRC-PCEST significantly enhanced the breakdown of PET, releasing more monomer TPA. In addition, Li et al. identified two BHETases (ChryBHETase and BsEst), which were combined as a two-enzyme system to yield up to 7.0-fold improved TPA production compared to seven state-of-the-art PET hydrolases [66]. Even for mixed or blended polymers containing PET, PBAT, and TPU, a dual-enzyme system consisting of the engineered polyester hydrolase PES-H1 FY and the urethanase SP2 could be used for depolymerization in a one-pot manner [67]. Complementary, our dual enzyme system addressed the depolymerization of polyether-polyester-based PUR for the first time. Combining cutinase HiC and urethanase SP2 achieved nearly 3-fold improved MDA monomer yield, which will certainly inform future efforts in the biological recycling and upcycling of PUR plastic wastes.

3.4 | Substrate Specificity of HiC Toward Three Building Blocks

In light of the structural complexity of the polyether-polyester-PUR, we intended to explore the substrate specificity of HiC toward the three repeating units (Figure 1). Molecular docking was used to understand the ligand-protein interactions of three representative building blocks (Figure 5) comprising the different repeating units of the PUR investigated (Figure 1). Key amino acid residues responsible for the enzyme-substrate interactions are shown in Figure 5.

Molecular docking is a well-established computational approach that has been extensively used for simulating and analyzing the interactions between small molecules and proteins. It offers significant advantages (e.g., rapid and cost-effective) over experimental methods such as X-ray diffraction, solution NMR, and electron microscopy [68]. Here, we used molecular docking to understand the different interactions between three monomeric units and the enzyme HiC. Several important amino acid residues responsible for the formation of hydrogen bonds, Pi-Alkyl, Pi-Sigma, and van der Waals interactions were uncovered. Two hydrogen bonds were found between building block 3 that contains the ester bond and HiC, while only one hydrogen bond was formed between the building blocks 1 and 2, comprising urethane units and the enzyme. Hydrogen bonds are highly pertinent to enzymatic catalysis, which contribute to the reaction by facilitating the formation of productive enzyme-substrate (ES) complexes and further stabilizing the transition state (TS) [69]. The single hydrogen bond formed between building block 1, 2, and the enzyme involved Tyr104 and His173 and the urethane NH (Figure 5a,b), while the two hydrogen bonds between enzyme and building block 3 involved the side chain NH_2 group of Asn69 and the side chain OH group of Ser105 (Figure 5c). Given that Ser105 is one of the catalytic residues of HiC (S105-D160-H173), forming the hydrogen bonds may assist it as a nucleophile attacking the carbonyl carbon in building block 3 to form a covalent bond, initiating a catalytic hydrolysis of ester bonds, and eventually releasing the compounds ① and ② introduced above. An energy minimization of this docked structure using YASARA [70] and the AMBER14 force-field [71] demonstrated a nucleophilic attack distance of 3.7 Å between the reacting Ser Oγ and the carbonyl carbon of the building block 3 (Figure S6).

More interestingly, both Asn69 and Ser105 form the hydrogen bonds through connection to the oxygen atoms in the ester bond, whereas Tyr104 and His173 form one hydrogen bond via the hydrogen atoms in the N-H part of MDA. The oxyanion hole is formed by the side chain of Ser28 and the backbone of Gln106, which stabilizes the negative charge of the tetrahedral TS during catalysis. Following nucleophilic attack on the *Si* face of the carbonyl carbon of building block 3, the oxyanion hole is formed. More stabilizing interactions facilitating the binding of building block 3 to the enzyme include Pi-alkyl formed by residues Tyr104 and Leu66, Pi-sigma by residues Ile169 and Leu174, as well as van der Waals interactions by residues Ser28, Thr29, Phe70, Thr135, Val162, Leu167, Ile168, and His173. This might explain the high preference of the enzyme toward the ester-bond hydrolysis. Still, it should be noted that a limitation of the docking approach used in this study is that the protein was treated as a rigid structure during the simulations, with only the catalytic triad (S105-D160-H173) set as flexible residues. Consequently, overall conformational flexibility of enzymes and potential induced-fit effects upon ligand binding were not explicitly considered, which may influence the accuracy of the predicted binding modes and affinities (Table S1).

3.5 | PUR Degradation by HiC and Its Two Mutants

Two HiC variants – the single-mutant (SM) I169Q and the double-mutant (DM) L66H/I169Q with enhanced promiscuous amidase activity and previously generated by us [72] – were employed to further improve the degradation efficiency. They were designed based on the hypothesis that introducing a hydrogen-bond acceptor to the scissile NH group of the substrate in the TS of HiC would increase the specificity toward amide groups. Specifically, L66 and I169 were identified as hotspot residues in HiC based on structural comparison of a corresponding TS model of prolyl oligopeptidase that share the same α,β-hydrolase fold and that displays a hydrogen bond to the reacting amide of its canonical substrate. Molecular modeling of the HiC mutants I169Q and I169Q/L66H indeed showed altered H-bonding interactions to the reactive bond in the substrate [72]. For this reason, we were interested to explore the impact of these mutations on performance of substrates that contain both C—O and C—N scissile bonds. The results in this study indicated that both HiC_SM and HiC_DM exhibited enhanced degradation activity against PUR films, with increased weight loss after 24 h incubation (Figure 6a). Docking studies demonstrated that Q169 of HiC_SM was able to form a hydrogen bond to one of the carbonyl oxygens in the ester part of the substrate, while both H66 and Q169 residues in HiC_DM contributed to the van der Waals interactions with building block 3 (Figure S7). When incubation time increased to 48 and 72 h, these two mutants showed a slight decrease in activity since the weight loss did not continuously increase with time (Figure 6b). This might be related to the reduced stability of the variants, which is also suggested by the detection of compounds ① and ② over time by HPLC analysis (Figure 6c).

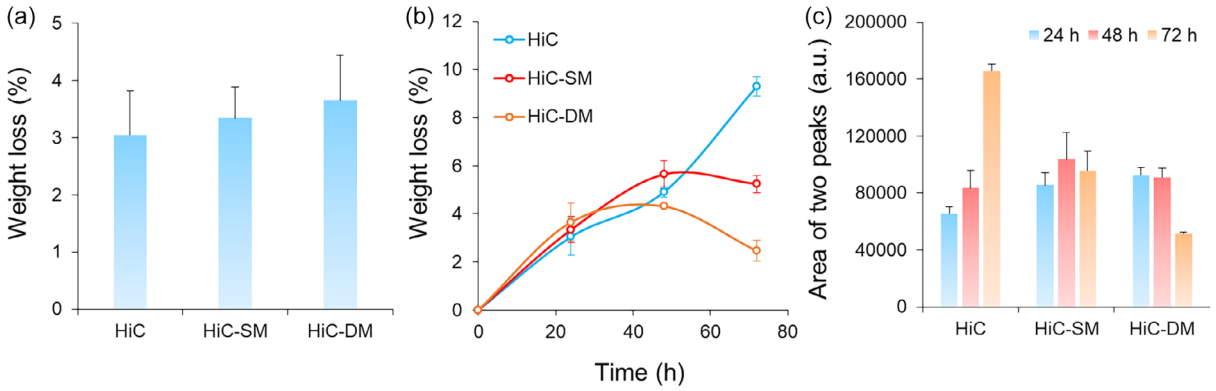

FIGURE 6 | Degradation of polyether-polyester-PUR films by HiC and two variants. (a) Weight loss of PUR films (particle loading of 15 mg/mL) after enzymatic reaction at 50°C for 24 h. The reaction system includes the same weight (~10 mg) of PUR films with a similar shape and 10 μg pure enzyme in Tris-HCl buffer (25 mM, pH 7.5). (b) Weight loss of PUR films with increasing time up to 72 h. (c) Calculation of the peak area of the two intermediates ① and ② (shown in Figure 4c) in HPLC spectra with time up to 72 h.

Our previous study showed that cutinase HiC hydrolyzed both ester and amide bonds in the substrates investigated. However, the hydrolysis of amide bonds was significantly slower than the cleavage of ester bonds. Satisfyingly, the two improved mutants (featuring an amidase-like hydrogen bond into the TS of cutinase HiC) showed a nearly 50-fold increase in hydrolysis of the amide over ester bond in *p*-nitrobutyranilide and *p*-nitrophenyl butyrate substrates, respectively, compared to the wild type enzyme [72]. Similar results were obtained in the study aiming at switching the substrate specificity of cutinases from *Thermobifida cellulosilytica* and *H. insolens* toward amide bond hydrolysis [73]. Through enzyme engineering, it was reported that a reallocated water network for hydrogen bond formation was generated to enhance the stabilization of the transition state during the enzymatic catalysis. When applied to polyamide hydrolysis, the HiC variants afforded increased catalytic efficiency.

In the present study, we also observed the increased degradation activity of HiC mutants toward the commercial PUR, with an increase in the weight loss of films. Compared to the HiC wild type, we assumed that the specific hydrogen bonds (HiC_SM: from sidechain of Q169 to the carbonyl oxygen of ester group and backbone C163 to the oxygen of urethane group; HiC_DM: side chain carbonyl of N69 accepting a hydrogen bond from the urethane group and S105 to the oxygen of ester bond) formed between the polymer substrate and HiC variants might help to stabilize the TS, and in turn lower the activation energy and increase the enzyme's activity. Effects on substrate association are also possible, and apart from altered hydrogen bonding patterns, additional interactions such as sulfur-X and π-lone pair formed by C163 and S28 with the building block 3 in HiC_SM, alkyl and π-lone pair formed by L174 and S28 with the substrate in HiC_DM might enhance the affinity toward the polymer. However, according to HPLC analysis, we did not observe the formation of the monomer MDA from PUR films. Even though these mutants displayed an enhanced hydrolysis activity toward amide bonds, it might still be difficult to hydrolyze the highly stable N-aryl carbamate bonds in PURs or the intermediate degradation products (e.g., ① and ②). Further analysis of the sites of the HiC_SM and HiC_DM demonstrated that I169 was located at the top loop structure of the protein (Figure S8). Since mutations in loop regions can increase flexibility and entropy, affecting the folding of enzymes, replacing the amino acid residues (from I to Q) might contribute to the decreased thermal stability [74]. Moreover, unlike rigid secondary structures such as α-helices and β-sheets, loops rely on a delicate balance of weak interactions (e.g., hydrogen bonds, hydrophobic contacts) to maintain their architecture. Mutations can easily disrupt these interactions, increase local flexibility, or cause misfolding, which in turn affects enzyme activity. Additionally, loops frequently participate in substrate binding or help position catalytic residues. Consequently, altering their amino acid composition can compromise both structural stability and proper active-site geometry, leading to reduced enzyme stability/activity. In the future, more efforts are needed to explore the residues responsible for the urethane bond hydrolysis and protein stability by using structure-based rational design. The resulting bifunctional enzyme would be expected to achieve enhanced- or even complete- depolymerization of PUR in an innovative and eco-friendly process.

4 | Conclusions

In the present study, we investigated the depolymerization of a commercial polyether-polyester-PUR through the combination of low-temperature thermal treatment and enzymatic cascade hydrolysis. The thermal pretreatment altered the structural properties of PUR, which were determined using UV–Vis, DSC, SEC, and FTIR techniques. Compared to other established methods like pyrolysis, solvolysis, and glycolysis, for example, low-temperature thermal pretreatment offers advantages, such as being solvent-free, reduced energy consumption and costs, simple operation independent of additional (metal) catalysts, and being environmentally friendly. Moreover, it might be applicable prior to the large-scale depolymerization of postconsumer plastic wastes and will be further investigated in the future, together with an optimization of heat pretreatment conditions.

The enzymatic hydrolysis enabled increased weight loss with time, which could be confirmed by surface modifications of PUR films. Two degradation products were identified using HPLC-MS after incubation with cutinase HiC for 24 h. Furthermore, the addition of the urethanase SP2 achieved the

depolymerization of PUR into its constituent monomer MDA. A 3-fold increase in the MDA monomer yield was obtained when compared to using the urethanase SP2 alone. Molecular docking indicated the high substrate specificity of HiC toward ester bond-containing building block 3 inside the polymeric units, with two hydrogen bonds formed. In addition, two previously established HiC variants exhibited increased degradation activity against PUR films within 24 h. Overall, this study provides an advanced concept for the depolymerization of polyether-polyester-PUR, with great potential for industrial applications in the recycling of PUR plastic waste and beyond.

Acknowledgments

The authors acknowledge funding from the Carl Trygger Foundation (CTS 23:2626), the FORMAS agency (2021–02509), and the Novo Nordisk Foundation (projects #NNF23OC0086236 and projects #PolyFine).

Funding

This study was supported by Carl Tryggers Stiftelse för Vetenskaplig Forskning (CTS 23:2626); Svenska Forskningsrådet Formas (2021–02509); Novo Nordisk Fonden (NNF23OC0086236, NNF25OC0100562), the National Academic Infrastructure for Supercomputing in Sweden (NAISS), Swedish Research Council (VR) (2022−06725) and the PDC Centre for High Performance Computing at the Royal Institute of Technology and SNIC and NAISS (NAISS 2025/5-398, NAISS 2025/23-373),.

Conflicts of Interest

The authors declare no conflicts of interest.

Data Availability Statement

Supporting information is available. Raw data will be made open accessible in Zenodo upon acceptance.

References

1. A. Das and P. Mahanwar, "A Brief Discussion on Advances in Polyurethane Applications," *Advanced Industrial and Engineering Polymer Research* 3 (2020): 93–101.

2. S. P. Katnic and R. K. Gupta, "From Biofilms to Biocatalysts: Innovations in Plastic Biodegradation for Environmental Sustainability," *Journal of Environmental Management* 374 (2025): 124192.

3. G. Rossignolo, G. Malucelli, and A. Lorenzetti, "Recycling of Polyurethanes: Where We Are and where We Are Going," *Green Chemistry* 26 (2024): 1132–1152.

4. E. Zarezadeh, M. Tangestani, and A. J. Jafari, "A Systematic Review of Methodologies and Solutions for Recycling Polyurethane Foams to Safeguard the Environment," *Heliyon* 10 (2024): e40724.

5. P. Bhavsar, M. Bhave, and H. K. Webb, "Solving the Plastic Dilemma: the Fungal and Bacterial Biodegradability of Polyurethanes," *World Journal of Microbiology and Biotechnology* 39 (2023): 122.

6. V. Tournier, S. Duquesne, F. Guillamot, et al., "Enzymes' Power for Plastics Degradation," *Chemical Reviews* 123 (2023): 5612–5701.

7. J. Ru, Y. Huo, and Y. Yang, "Microbial Degradation and Valorization of Plastic Wastes," *Frontiers in Microbiology* 11 (2020): 442.

8. A. Delavarde, G. Savin, P. Derkenne, et al., "Sustainable Polyurethanes: Toward New Cutting-Edge Opportunities," *Progress in Polymer Science* 151 (2024): 101805.

9. J. Mallouhi, B. Viskolcz, E. Szőri-Dorogházi, and B. Fiser, *Hungarian Materials and Chemical Sciences and Engineering* 47 (2023): 100–108.

10. P. Król, "Synthesis Methods, Chemical Structures and Phase Structures of Linear Polyurethanes. Properties and Applications of Linear Polyurethanes in Polyurethane Elastomers, Copolymers and Ionomers," *Progress in Materials Science* 52 (2007): 915–1015.

11. J. Xu, W. Xiao, S. Zhang, Z. Dong, and C. Lei, "Synthesis and Characterization of Polyurethane with Poly(ether-Ester) Diols Soft Segments Consisted by ether and Ester Linkages in One Repeating Unit," *European Polymer Journal* 179 (2022): 111553.

12. S. Li, Z. Liu, L. Hou, Y. Chen, and T. Xu, "Effect of Polyether/Polyester Polyol Ratio on Properties of Waterborne Two-Component Polyurethane Coatings," *Progress in Organic Coatings* 141 (2020): 105545.

13. Y.-H. Liao and Y.-C. Chen, "Preparation and Optimization of WPU Dispersion from Polyether/Polyester Polyols for Film and Coating Applications," *Journal of the Taiwan Institute of Chemical Engineers* 145 (2023): 104832.

14. J. Liu, Q. Zeng, H. Lei, et al., "Biodegradation of Polyester Polyurethane by Cladosporium sp. P7: Evaluating Its Degradation Capacity and Metabolic Pathways," *Journal of Hazardous Materials* 448 (2023): 130776.

15. T. Bayer, G. J. Palm, L. Berndt, et al., "Structural Elucidation of a Metagenomic Urethanase and Its Engineering Towards Enhanced Hydrolysis Profiles," *Angewandte Chemie International Edition* 63 (2024): e202404492.

16. Y. Branson, S. Söltl, C. Buchmann, et al., *Angewandte Chemie International Edition* 62 (2023): e202216220.

17. Z. Li, X. Han, L. Cong, et al., "Structure-Guided Engineering of a Versatile Urethanase Improves Its Polyurethane Depolymerization Activity," *Advanced Science* 12 (2025): 2416019.

18. M. C. Krueger, H. Harms, and D. Schlosser, "Prospects for Microbiological Solutions to Environmental Pollution with Plastics," *Applied Microbiology and Biotechnology* 99 (2015): 8857–8874.

19. M. Muñoz-Martí, V. N. Bañón, M. C. García-Poyo, et al., "Isolation, Identification, and Characterization of Novel Environmental Bacteria with Polyurethane-Degrading Activity," *Biology* 14 (2025): 1307.

20. A. Soto-Hernández, L. F. Muriel-Millán, A. Gracia, A. Sánchez-Flores, and L. Pardo-López, "Enzymatic Characterization and Polyurethane Biodegradation Assay of Two Novel Esterases Isolated from a Polluted River," *PLoS One* 20 (2025): e0327637.

21. J. Ru, X. Chen, X. Dong, L. Hu, J. Zhang, and Y. Yang, "Discovery of a Polyurethane-Degrading Enzyme from the Gut Bacterium of Plastic-Eating Mealworms," *Journal of Hazardous Materials* 480 (2024): 136159.

22. J. Liu, J. He, R. Xue, et al., "Biodegradation and up-Cycling of Polyurethanes: Progress, Challenges, and Prospects," *Biotechnology Advances* 48 (2021): 107730.

23. L. Zhang, K. Cao, H. Liu, et al., "Discovery of a Polyester Polyurethane-Degrading Bacterium from a Coastal Mudflat and Identification of Its Degrading Enzyme," *Journal of Hazardous Materials* 483 (2025): 136659.

24. S. Khruengsai, T. Sripahco, and P. Pripdeevech, "Biodegradation of Polyester Polyurethane by Embarria Clematidis," *Frontiers in Microbiology* 13 (2022): 874842.

25. Z. Shah, M. Gulzar, F. Hasan, and A. A. Shah, "Degradation of Polyester Polyurethane by an Indigenously Developed Consortium of Pseudomonas and Bacillus Species Isolated from Soil," *Polymer Degradation and Stability* 134 (2016): 349–356.

26. S. H. Lee, H. Jeong, I. Jung, M. Choi, and A.-R. Kim, "Characterization of Newly Discovered Polyester Polyurethane-Degrading, *Methylobacterium Aquaticum*, Strain A1," *Journal of Basic Microbiology* 65 (2025): e70066.

27. K. Świderek, K. Arafet, V. de Sousa Batista, D. Grajales-Hernández, F. López-Gallego, and V. Moliner, *Journal of the American Chemical Society* 147 (2025): 42511–42523.

28. Y. Chen, J. Sun, K. Shi, et al., "Glycolysis-Compatible Urethanases for Polyurethane Recycling," *Science* 390 (2025): 503–509.

29. S. Sun and P.-O. Syrén, "Chemoenzymatic Cascade Depolymerization of Plastics," *Communications Chemistry* 8 (2025): 272.

30. P. Scholz, V. Wachtendorf, U. Panne, and S. M. Weidner, "Degradation of MDI-Based Polyether and Polyester-Polyurethanes in Various Environments - Effects on Molecular Mass and Crosslinking," *Polymer Testing* 77 (2019): 105881.

31. O. Trott and A. J. Olson, "AutoDock Vina: Improving the Speed and Accuracy of Docking with a New Scoring Function, Efficient Optimization, and Multithreading," *Journal of Computational Chemistry* 31 (2010): 455–461.

32. M. D. Hanwell, D. E. Curtis, D. C. Lonie, T. Vandermeersch, E. Zurek, and G. R. Hutchison, "Avogadro: An Advanced Semantic Chemical Editor, Visualization, and Analysis Platform," *Journal of Cheminformatics* 4 (2012): 17.

33. G. M. Morris, R. Huey, W. Lindstrom, et al., "AutoDock4 and AutoDockTools4: Automated Docking with Selective Receptor Flexibility," *Journal of Computational Chemistry* 30 (2009): 2785–2791.

34. Q. Dong, A. D. Lele, X. Zhao, et al., "Depolymerization of Plastics by Means of Electrified Spatiotemporal Heating," *Nature* 616 (2023): 488–494.

35. R. M. O'Dea, M. Nandi, G. Kroll, J. R. Arnold, L. T. J. Korley, and T. H. Epps, "III, Toward Circular Recycling of Polyurethanes: Depolymerization and Recovery of Isocyanates," *JACS Au* 4 (2024): 1471–1479.

36. S. H. Ji, D. C. Seok, and S. Yoo, *Environmental Technology & Innovation* 32 (2023): 103449.

37. R. E. Marchant, Q. Zhao, J. M. Anderson, and A. Hiltner, "Degradation of a Poly(ether Urethane Urea) Elastomer: Infra-Red and XPS Studies," *Polymer* 28 (1987): 2032–2039.

38. K. Bruckmoser and K. Resch, "Investigation of Ageing Mechanisms in Thermoplastic Polyurethanes by Means of IR and Raman Spectroscopy," *Macromolecular Symposia* 339 (2014): 70–83.

39. R. Kirchner and H. Schift, "Thermal Reflow of Polymers for Innovative and Smart 3D Structures: A Review," *Materials Science in Semiconductor Processing* 92 (2019): 58–72.

40. I. Yilgor, E. Yilgor, I. G. Guler, T. C. Ward, and G. L. Wilkes, "FTIR Investigation of the Influence of Diisocyanate Symmetry on the Morphology Development in Model Segmented Polyurethanes," *Polymer* 47 (2006): 4105–4114.

41. J. T. Garrett, R. Xu, J. Cho, and J. Runt, "Phase Separation of Diamine Chain-Extended Poly(urethane) Copolymers: FTIR Spectroscopy and Phase Transitions," *Polymer* 44 (2003): 2711–2719.

42. D. Im, V. Gavande, H. Y. Lee, and W.-K. Lee, "Influence of Molecular Weight on the Enzymatic Degradation of PLA Isomer Blends by a Langmuir System," *Materials* 16 (2023): 5087.

43. Z. Hou, P. Li, J. Guo, J. Wang, J. Hu, and L. Yang, "The Effect of Molecular Weight on Thermal Properties and Degradation Behavior of Copolymers Based on TMC and DTC," *Polymer Degradation and Stability* 175 (2020): 109128.

44. A. Chamas, H. Moon, J. Zheng, et al., "Degradation Rates of Plastics in the Environment," *ACS Sustainable Chemistry & Engineering* 8 (2020): 3494–3511.

45. R. Gallorini, B. Ciuffi, F. Real Fernández, et al., "Subcritical Hydrothermal Liquefaction as a Pretreatment for Enzymatic Degradation of Polyurethane," *ACS Omega* 7 (2022): 37757–37763.

46. S. Chen, L. Su, J. Chen, and J. Wu, "Cutinase: Characteristics, Preparation, and Application," *Biotechnology Advances* 31 (2013): 1754–1767.

47. Q. Huang, S. Kimura, and T. Iwata, "Thermal Embedding of, *Humicola Insolens*, Cutinase: A Strategy for Improving Polyester Biodegradation in Seawater," *Biomacromolecules* 24 (2023): 5836–5846.

48. E. d. Q. Eugenio, I. S. P. Campisano, A. M. de Castro, M. A. Z. Coelho, and M. A. P. Langone, "Kinetic Modeling of the Post-Consumer Poly(Ethylene Terephthalate) Hydrolysis Catalyzed by Cutinase from Humicola Insolens," *Journal of Polymers and the Environment* 30 (2022): 1627–1637.

49. A. Wu, F. Sha, S. Su, and O. K. Farha, "Recyclable Enzymatic Hydrolysis with Metal-Organic Framework Stabilized Humicola Insolens Cutinase (HiC) for Potential PET Upcycling," *Chem & Bio Engineering* 1 (2024): 798–804.

50. S. Kaabel, J. P. D. Therien, C. E. Deschênes, D. Duncan, T. Friščić, and K. Auclair, "Enzymatic Depolymerization of Highly Crystalline Polyethylene Terephthalate Enabled in Moist-Solid Reaction Mixtures," *Proceedings of the National Academy of Sciences* 118 (2021): e2026452118.

51. F. Di Bisceglie, F. Quartinello, R. Vielnascher, G. M. Guebitz, and A. Pellis, "Cutinase-Catalyzed Polyester-Polyurethane Degradation: Elucidation of the Hydrolysis Mechanism," *Polymers* 14 (2022): 411.

52. S.-Y. Fu, X.-Q. Feng, B. Lauke, and Y.-W. Mai, "Effects of Particle Size, Particle/Matrix Interface Adhesion and Particle Loading on Mechanical Properties of Particulate–polymer Composites," *Composites Part B: Engineering* 39 (2008): 933–961.

53. H. Lu, D. J. Diaz, N. J. Czarnecki, et al., "Machine Learning-Aided Engineering of Hydrolases for PET Depolymerization," *Nature* 604 (2022): 662–667.

54. B. C. Almeida, P. Figueiredo, and A. T. P. Carvalho, "Polycaprolactone Enzymatic Hydrolysis: A Mechanistic Study," *ACS Omega* 4 (2019): 6769–6774.

55. H. R. Amedi and M. Aghajani, "Gas Separation in Mixed Matrix Membranes Based on Polyurethane Containing SiO.2, ZSM-5, and ZIF-8 Nanoparticles," *Journal of Natural Gas Science and Engineering* 35 (2016): 695–702.

56. T. H. Nguyen, A. R. Padalhin, H. S. Seo, and B. T. Lee, "A Hybrid Electrospun PU/PCL Scaffold Satisfied the Requirements of Blood Vessel Prosthesis in Terms of Mechanical Properties, Pore Size, and Biocompatibility," *Journal of Biomaterials Science, Polymer Edition* 24 (2013): 1692–1706.

57. C. M. Silva, F. Carneiro, A. O'Neill, et al., "Cutinase-A New Tool for Biomodification of Synthetic Fibers," *Journal of Polymer Science, Part A: Polymer Chemistry* 43 (2005): 2448–2450.

58. Z. Jiang, X. Chen, H. Xue, et al., "Novel Polyurethane-Degrading Cutinase BaCut1 from Blastobotrys sp. G-9 with Potential Role in Plastic Bio-Recycling," *Journal of Hazardous Materials* 472 (2024): 134493.

59. J. Liu, K. Xin, T. Zhang, et al., "Identification and Characterization of a Fungal Cutinase-Like Enzyme CpCut1 from Cladosporium sp. P7 for Polyurethane Degradation," *Applied and Environmental Microbiology* 90 (2024): e01477–01423.

60. A. Roman Victor, R. Crable Bryan, N. Wagner Dominique, et al., "Identification and Recombinant Expression of a Cutinase from Papiliotrema Laurentii that Hydrolyzes Natural and Synthetic Polyesters," *Applied and Environmental Microbiology* 90 (2024): e01694–01623.

61. A. Raczyńska, A. Góra, and I. André, "An Overview on Polyurethane-Degrading Enzymes," *Biotechnology Advances* 77 (2024): 108439.

62. S. P. Katnic, F. M. de Souza, and R. K. Gupta, "Recent Progress in Enzymatic Degradation and Recycling of Polyurethanes," *Biochemical Engineering Journal* 208 (2024): 109363.

63. K. Xin, J. Lu, Q. Zeng, et al., "Depolymerization of the Polyester–polyurethane by Amidase GatA250 and Enhancing the Production of 4,4′-Methylenedianiline with Cutinase LCC," *Biotechnology Journal* 19 (2024): 2300723.

64. B. C. Knott, E. Erickson, M. D. Allen, et al., "Characterization and Engineering of a Two-Enzyme System for Plastics Depolymerization," *Proceedings of the National Academy of Sciences* 117 (2020): 25476–25485.

65. J. Sun, Y. Pang, Z. Lei, et al., "Enzymatic Depolymerization of Plastic Materials by a Highly Efficient Two-Enzyme System," *Biochemical Engineering Journal* 204 (2024): 109222.

66. A. Li, Y. Sheng, H. Cui, et al., "Discovery and Mechanism-Guided Engineering of BHET Hydrolases for Improved PET Recycling and Upcycling," *Nature Communications* 14 (2023): 4169.

67. Y. Branson, J. Liu, L. Schmidt, et al., "One-Pot Depolymerization of Mixed Plastics Using a Dual Enzyme System," *ChemSusChem* 18 (2025): e202402416.

68. M. Mohanty and P. S. Mohanty, "Molecular Docking in Organic, Inorganic, and Hybrid Systems: A Tutorial Review," *Monatshefte für Chemie - Chemical Monthly* 154 (2023): 683–707.

69. L. I. Matienko, E. M. Mil, A. A. Albantova, and A. N. Goloshchapov, "The Role H-Bonding and Supramolecular Structures in Homogeneous and Enzymatic Catalysis," *International Journal of Molecular Sciences* 24 (2023): 16874.

70. H. Land and M. S. Humble, *Protein Engineering: Methods and Protocols*, ed. U. T. Bornscheuer and M. Höhne (Springer, 2018), 43–67.

71. J. A. Maier, C. Martinez, K. Kasavajhala, L. Wickstrom, K. E. Hauser, and C. Simmerling, "ff14SB: Improving the Accuracy of Protein Side Chain and Backbone Parameters from ff99SB," *Journal of Chemical Theory and Computation* 11 (2015): 3696–3713.

72. P.-O. Syrén, P. Hendil-Forssell, L. Aumailley, et al., "Esterases with an Introduced Amidase-Like Hydrogen Bond in the Transition State Have Increased Amidase Specificity," *ChemBiochem* 13 (2012): 645–648.

73. A. Biundo, R. Subagia, M. Maurer, D. Ribitsch, P.-O. Syrén, and G. M. Guebitz, "Switched Reaction Specificity in Polyesterases towards Amide Bond Hydrolysis by Enzyme Engineering," *RSC Advances* 9 (2019): 36217–36226.

74. R. Guzzi, L. Sportelli, S. Yanagisawa, C. Li, D. Kostrz, and C. Dennison, "The Influence of Active Site Loop Mutations on the Thermal Stability of Azurin from Pseudomonas Aeruginosa," *Archives of Biochemistry and Biophysics* 521 (2012): 18–23.

Supporting Information

Additional supporting information can be found online in the Supporting Information section. **Supporting Fig. S1:** SDS-PAGE of purified enzymes. (a) WT: wild-type HiC, SM: single mutation = I169Q, and DM: double mutation = L66H/I169Q. (b) Purified urethanase SP2 from different wells in the fraction collector of ÄKTA. **Supporting Fig. S2:** Standard curve of MDA. (a) HPLC spectra of different concentrations of MDA (0.0005-5 mM). Retention time of MDA is at 1.983 min. (b) Linear standard curve of MDA (concentration vs. peak area). **Supporting Fig. S3:** Solubility test of PUR before and after heat treatment. (a) Representative images of PUR samples with different particle loads (from 2.5 to 15 mg/mL) in THF. "Un" stands for the untreated PUR samples, and "T" indicates the heat-treated samples. (b) Solubility of untreated PUR and heat-treated PUR in THF. All samples were dissolved in 20 mL THF at room temperature overnight. The insoluble residues were subsequently collected using centrifugation at 5,000 *g* and 20°C for 15 min, dried in the fume hood for 24 h, and weighed for calculating the solubility (g per 100 g THF). **Supporting Fig. S4:** Measurement of the thickness of PUR film before and after heat pretreatment. **Supporting Fig. S5:** Possible structure of compound ① with *m/z* of 532.20 in its ammonium-complexed form ($[M+NH_4]^+$; $m = 18.04$ g/mol). Molecular weight of compound ① is 514.20. **Supporting Fig. S6:** Analysis of a docked energy-minimized structure by YASARA. It shows a nucleophilic attack distance of 3.7 Å between the reacting Ser Oγ of the cutinase HiC and the carbonyl carbon of the building block 3. **Supporting Fig. S7:** Docking results of HIC_SM (a) and HIC_DM (b) with building block 3. Interactions between the substrate (building block 3) and the two mutants' residues were identified in different colors. **Supporting Fig. S8:** Positions of residues L66 and I169 in the structure of HiC (PDB ID: 4OYY). **Supporting Table S1:** Selected poses of three PUR building blocks after docking.